FERMILAB-FN-1085-A

Research and Development for HI Intensity Mapping

Thematic Areas: Technological Development Activity, Ground Based Project

Primary Contact:
Name: Peter Timbie
Institution: UW-Madison
Email: pttimbie@wisc.edu
Phone: 608-890-2002

Abstract: Development of the hardware, data analysis, and simulation techniques for large compact radio arrays dedicated to mapping the 21 cm line of neutral hydrogen gas has proven to be more difficult than imagined twenty years ago when such telescopes were first proposed. Despite tremendous technical and methodological advances, there are several outstanding questions on how to optimally calibrate and analyze such data. On the positive side, it has become clear that the outstanding issues are purely technical in nature and can be solved with sufficient development activity. Such activity will enable science across redshifts, from early galaxy evolution in the pre-reionization era to dark energy evolution at low redshift.

Contributors and Endorsers: Zeeshan Ahmed[1], David Alonso[2], Mustafa A. Amin[3], Réza Ansari[4], Evan J. Arena[5,6], Kevin Bandura[7,8], Adam Beardsley[9], Philip Bull[10,11], Emanuele Castorina[12], Tzu-Ching Chang[13], Romeel Davé[14], Alexander van Engelen[15,9], Aaron Ewall-Wice[13], Simone Ferraro[16], Simon Foreman[15], Josef Frisch[1], Daniel Green[17], Gilbert Holder[18], Daniel Jacobs[9], Joshua S. Dillon[19], Dionysios Karagiannis[20,21], Alexander A. Kaurov[22], Lloyd Knox[23], Emily Kuhn[24], Adrian Liu[25], Yin-Zhe Ma[26], Kiyoshi W. Masui[27], Thomas McClintock[5], Kavilan Moodley[26], Moritz Münchmeyer[28], Laura B. Newburgh[24], Andrei Nomerotski[5], Paul O'Connor[5], Andrej Obuljen[29], Hamsa Padmanabhan[15], David Parkinson[30], Olivier Perdereau[4], David Rapetti[31,32], Benjamin Saliwanchik[24], Neelima Sehgal[33], J. Richard Shaw[34], Chris Sheehy[5], Erin Sheldon[5], Raphael Shirley[35], Eva Silverstein[36], Tracy Slatyer[27,22], Anže Slosar[5], Paul Stankus[5], Albert Stebbins[37], Peter T. Timbie[38], Gregory S. Tucker[39], William Tyndall[5,24], Francisco Villaescusa-Navarro[40], Dallas Wulf[25]

[1] SLAC National Accelerator Laboratory, Menlo Park, CA 94025
[2] The University of Oxford, Oxford OX1 3RH, UK
[3] Department of Physics & Astronomy, Rice University, Houston, Texas 77005, USA
[4] Université Paris-Sud, LAL, UMR 8607, F-91898 Orsay Cedex, France & CNRS/IN2P3, F-91405 Orsay, France
[5] Brookhaven National Laboratory, Upton, NY 11973
[6] Drexel University, Philadelphia, PA 19104
[7] CSEE, West Virginia University, Morgantown, WV 26505, USA
[8] Center for Gravitational Waves and Cosmology, West Virginia University, Morgantown, WV 26505, USA
[9] Arizona State University, Tempe, AZ 85287

This manuscript has been authored by Fermi Research Alliance, LLC under Contract No. DE-AC02-07CH11359 with the U.S. Department of Energy, Office of Science, Office of High Energy Physics.

[10] Queen Mary University of London, Mile End Road, London E1 4NS, United Kingdom
[11] Department of Physics & Astronomy, University of the Western Cape, Cape Town 7535, South Africa
[12] Department of Physics, University of California Berkeley, Berkeley, CA 94720, USA
[13] Jet Propulsion Laboratory, California Institute of Technology, Pasadena, CA, USA
[14] University of Edinburgh, EH8 9YL Edinburgh, United Kingdom
[15] Canadian Institute for Theoretical Astrophysics, University of Toronto, Toronto, ON M5S 3H8, Canada
[16] Lawrence Berkeley National Laboratory, Berkeley, CA 94720
[17] University of California San Diego, La Jolla, CA 92093
[18] Department of Physics, University of Illinois at Urbana-Champaign, Urbana, Illinois 61801, USA
[19] Department of Astronomy, University of California Berkeley, Berkeley, CA 94720, USA
[20] Dipartimento di Fisica e Astronomia "G. Galilei",Università degli Studi di Padova, via Marzolo 8, I-35131, Padova, Italy
[21] Istituto Nazionale di Fisica Nucleare, Sezione di Padova, via Marzolo 8, I-35131, Padova, Italy
[22] Institute for Advanced Study, Princeton, NJ 08540
[23] University of California at Davis, Davis, CA 95616
[24] Department of Physics, Yale University, New Haven, CT 06520
[25] McGill University, Montreal, QC H3A 2T8, Canada
[26] Astrophysics and Cosmology Research Unit, School of Chemistry and Physics, University of KwaZulu-Natal, Durban 4000, South Africa
[27] Massachusetts Institute of Technology, Cambridge, MA 02139
[28] Perimeter Institute, Waterloo, Ontario N2L 2Y5, Canada
[29] Centre for Astrophysics, University of Waterloo, Waterloo, Ontario N2L 3G1, Canada
[30] Korea Astronomy and Space Science Institute, Daejeon 34055, Korea
[31] Center for Astrophysics and Space Astronomy, Department of Astrophysical and Planetary Science, University of Colorado, Boulder, CO 80309, USA
[32] NASA Postdoctoral Program Senior Fellow, NASA Ames Research Center, Moffett Field, CA 94035, USA
[33] Stony Brook University, Stony Brook, NY 11794
[34] University of British Columbia, Vancouver, BC V6T 1Z1, Canada
[35] Instituto de Astrof íisica de Canarias, 38200 La Laguna, Tenerife, Spain
[36] Stanford University, Stanford, CA 94305
[37] Fermi National Accelerator Laboratory, Batavia, IL 60510
[38] Department of Physics, University of Wisconsin - Madison, Madison, WI 53706
[39] Brown University, Providence, RI 02912
[40] Center for Computational Astrophysics, 162 5th Ave, 10010, New York, NY, USA

1 Key Science Goals & Objectives

Three-dimensional surveys with the redshifted $21\,\mathrm{cm}$ line are key to achieving many of the goals outlined by Astro2020 Science White Papers. In the near future, this technique, called 21 *cm intensity mapping*, will likely surpass optical surveys in terms of volume of the cosmos surveyed. The science goals include: exploration of the cosmic Dark Ages, Cosmic Dawn and the Epoch of Reionization [1–9]; understanding inflation [9–12]; understanding dark energy and modified gravity [13]; and determining neutrino mass [14]. In addition, owing to their large fields of view and high survey speeds, many $21\,\mathrm{cm}$ intensity mapping instruments can simultaneously monitor the sky for transient events, such as pulsars and fast radio bursts (FRBs). Science white papers [15–17] outline plans to understand the FRB mechanism and use them as cosmological probes. And some intensity mapping instruments will discover new millisecond pulsars, essential for the improved pulsar timing arrays for gravitational wave detection, as described in white papers [18–23].

After the recombination of hydrogen, when the Cosmic Microwave Background (CMB) was created at redshifts around $z \sim 1150$, the baryonic portion of the universe was dominated by neutral hydrogen. As matter continued to cluster in the post-recombination universe, peaks in the matter density grew and eventually led to the formation of the first generation of stars and galaxies, which emitted radiation capable of reionizing the ambient neutral hydrogen. Between recombination and the formation of the first stars, during the high-redshift epoch generally referred to as the Dark Ages ($30 \lesssim z \lesssim 150$), neutral hydrogen traces the overall matter distribution. $21\,\mathrm{cm}$ intensity mapping is the only known technique for accessing this epoch and could provide large-scale tomographic maps sampling vastly more of the pristine density fluctuation modes than can the CMB.

Later, between $z \sim 30$ and $z \sim 6$, first-generation stars and galaxies formed and began the process of reionizing the universe. During this epoch, including Cosmic Dawn and the Epoch of Reionization (EoR), the signal is boosted by large regions of completely ionized "bubbles" residing in a sea of otherwise largely neutral hydrogen. Probing this unexplored phase of cosmic evolution was the top-ranked science program from the Astro2010 Radio, Millimeter, and Submillimeter panel. Indeed, a number of experiments, such as LWA, HERA, PAPER, LOFAR, MWA, and GMRT, are seeking to make the first measurements of how the first luminous objects affected the large-scale distribution and ionization state of hydrogen. They are spurred on by the possible detection of the signature of the formation of the first stars in the global spectrum [24] (as opposed to maps) of the $21\,\mathrm{cm}$. Because CMB photons scatter from the ionized matter, these intensity mapping measurements are critical to interpreting CMB power spectra. In particular, they can provide independent (of the CMB) measurements of τ, the optical depth of reionization, which is required for CMB constraints on neutrino mass [25].

Finally, in the post-EoR epoch, $z \lesssim 6$, the universe is mostly ionized, with a few pockets of neutral hydrogen residing in galaxies. $21\,\mathrm{cm}$ intensity mapping can measure the large scale structure in this epoch by surveying the aggregate emission from many unresolved galaxies. Even without resolving individual objects, one can still trace the fluctuations in their number density across space and redshift on large scales, where theoretical modeling is most robust. A key goal is to determine the expansion history of the universe spanning redshifts $z = 0.3 - 6$, complementing existing measurements at low redshift while opening up new windows at high redshifts. Another goal is to measure the growth-rate of structure formation over this same wide range of redshift and thus constrain modifications of gravity over a wide range of scales and times in cosmic history. One can also observe, or constrain, the presence of inflationary relics in the primordial power spectrum and observe, or constrain, primordial non-Gaussianity. The first generation of experiments in this redshift range include GBT, CHIME, Tianlai, HIRAX, OWFA, BINGO, BMX, and PAON. The proposed PUMA experiment [26] targets these science goals over the entire post-EoR epoch. Many of these instruments also include hardware and software for detecting radio transients. CHIME, for example, has already detected 13 FRBs [27] and is expected to find many more.

Reaching these science goals will require overcoming several challenges, including observing the 21 cm line over an enormous range of frequencies, from $\sim 10 - 1400$ MHz. However, all current observational programs, from Cosmic Dawn/EoR to post-EoR, have converged on broadly similar approaches. As outlined below, they require continued development of common hardware, data analysis, and simulation techniques. (A whitepaper focusing on Cosmic Dawn/EoR complements much of the discussion here [28].) Lessons learned from these ongoing programs will open wide a new window for astrophysics and cosmology.

2 Measurement Overview

Measuring the 21 cm signature of large scale structure promises enormous scientific payoffs. Unfortunately, the signal amplitude is small. These large volume surveys exploit large bandwidths, large fields of view, long integration times, and large numbers of receivers to maximize mapping speed. Over the past decade, measurements have evolved from using shared-facility single-dish radio telescopes and interferometers to dedicated 21 cm radio interferometers. Unlike facility interferometers (e.g. SKA), which include a mix of long and short baselines for high angular resolution imaging, intensity mapping interferometers are close-packed in order to map large-scale cosmological features. The recent revolution in low-noise radio technology allows the construction of relatively inexpensive interferometric arrays with hundreds to thousands of elements, bandwidth $\gtrsim 100$ MHz, and correlators powerful enough to process the signals from them. However, R&D can be carried out efficiently with small demonstrators, with on order ten elements. (See Table 1).

So far, Cosmic Dawn/EoR experiments have set upper limits on the 21 cm power spectrum [29,30]. These limits have steadily improved with better understanding and control of systematic effects. Post-EoR experiments have detected the 21 cm power spectrum in cross-correlation with galaxy redshift surveys [31–34] but none has so far detected it in autocorrelation, i.e. without the assistance of an optical galaxy redshift survey. These experiments face several measurement challenges, which we describe here. Later we outline how to overcome them with a coherent development plan.

Astrophysical foregrounds. Astrophysical foregrounds, primarily synchrotron emission from the Galaxy and unresolved point sources, pose the most significant measurement challenge, having much higher intensity than the 21 cm signal at all frequencies. These foregrounds have a smooth spectral shape and hence can in principle be distinguished from the 21 cm emission from large scale structure [35–38]. However, any frequency dependence in the instrument response, for example from the instrument beam or gain fluctuations, can complicate separation of the smooth foreground and the 'spikey' 21 cm signal [39, 40]. Removing these foregrounds drives most instrument design choices including array element uniformity, cross-polarization response, etc.

Instrument calibration. Each antenna has a characteristic response to an input sky signal, known as the instrument gain, which varies with both time and frequency. Each antenna also has a characteristic response on the sky, known as the instrument beam pattern. The gain and beam patterns must be measured well enough to remove astrophysical foreground power. Even in a 'perfect' instrument, the beam varies with frequency and causes features to appear in the spectrum that masquerade as structures in redshift space. If the frequency-dependent instrument response is known, these foregrounds can, in principle, be subtracted [41]. For actual post-EoR experiments, simulations for CHIME have provided a scale to the problem: the instrument response on the sky ('beam') must be understood to 0.1%, and the time-dependent response of the instrument ('gain') must be calibrated to 1% [39, 40]. Uniformity and stability specifications must be carefully integrated into the instrument design and verified during testing and deployment.

FFT beamforming, real time calibration, redundant baselines, and array redundancy. For current arrays, with up to about 1000 elements, one can compute the fundamental observables of an interferometer, the correlations of RF signals from pairs of antennas (visibilities), for all pairs, using existing correlator designs. Calibration occurs offline. However, the correlation cost and data rate from future, larger arrays will require implementing other correlators, such as the EPIC correlator [42], or FFT beamforming correlators. Both use FFT-based sampling of the interferometric geometry [43–46] to reduce the computational correlation cost, from order N^2 to $N \log N$ and output data volume from N^2 to order N. Although promising first steps with EPIC and FFT beamforming [42, 47] have been taken, they have not yet been demonstrated for 21 cm intensity mapping.

FFT beamforming in particular requires that all elements of the array be redundant (that their beams be similar), placing tight requirements on element uniformity. In addition, this correlation is performed in real time, and so requires real-time calibration to account for instrumental changes (or that the instrument remain extremely stable). Real-time calibration schemes are being developed [48]. Some exploit the fact that similar interferometric baselines should see the same sky signal and so differences between them can be used to assess relative instrument gains over time. This technique, known as 'redundant baseline' calibration [49–54], requires uniform interferometric elements with uniform spacing. And while promising, redundant baseline calibration has not yet been demonstrated to be good enough for 21 cm intensity mapping [55, 56].

Environmental considerations. In addition to astrophysical foregrounds, two terrestrial contaminants must be eliminated or otherwise mitigated: human-generated radio-frequency interference (RFI) and the ionosphere. Radio bands within the entire range of 21 cm redshifts are popular for communications. RFI appears at discrete frequencies and can be reduced or eliminated by a suitable choice of radio-quiet observation site [57]. Even experiments operating in locations with high degrees of interference, notably LOFAR (located in the Netherlands), have developed impressive RFI removal algorithms [58].

The ionospheric plasma disturbs long wavelength measurement through both refraction and Faraday rotation [59, 60]. The ionosphere acts in concert with the Earth's magnetic field to rotate the polarization vector of incoming light by Faraday rotation. The rotation is proportional to λ^2 as well as the number of free electrons present in the ionosphere, which varies across all time scales. While the 21 cm signal is unpolarized, most foreground emission from the Galaxy is polarized and adds a time-variable component to the foreground characterization and removal. The λ^2 dependence means it primarily affects experiments at longer wavelengths (frequencies below $\sim$ 500 MHz, $\sim z > 2$), which attempt to measure and remove this rotation using accurate maps of the magnetic field and GPS data to infer free electron content. Because signal propagation through the ionosphere is critical for satellite telecommunications, it is well modelled and current low frequency radio telescopes are working to remove signal variability from the ionosphere [61]. At even lower frequencies ionospheric refraction, which also scales with λ^2, probably becomes the dominant effect .

Required sensitivity. In the absence of systematic effects, detecting the 21 cm signal requires fielding instruments including thousands of receivers to reach the mean brightness temperature of the cosmological 21 cm signal of $\sim$ 0.1 - 1 mK within a few years. Instrument noise stems from a combination of intrinsic amplifier noise (noise temperatures for state-of-the-art radio telescopes range from 25 K cryogenic to 100 K uncooled) and sky brightness temperature (which span between 10 K - 1000 K depending on pointing and frequency). Because synchrotron emission increases at lower frequencies, at high redshifts (above $z \sim 3$) the system noise is dominated by the sky and no longer by the amplifier; improved sensitivity must be achieved by fielding more antennas rather than better performing front-end amplifiers.

Computing scale. Radio astronomy has always been at the forefront of 'big data' in astronomy. Current generation 21 cm instruments produce $\gtrsim 100\,\text{TB}$ of data per day without any compression. The data volume $\propto N^2$ where N is the number of elements (currently $N \sim 10^3$), representing challenges in data reduction, transfer, storage, analysis, distribution, and simulation. Compression by a factor of $\sim N$ is achievable with the FFT beamforming mentioned above. To aid in data transport, analysis, and data quality assessment, data must be compressed further (e.g. co-adding maps in a weekly cadence). This reduces the data size but increases pressure on real-time instrument calibration. In addition, to enable transient science, fast triggers are deployed at some current generation instruments [27].

3 Technology/hardware Development

Some of these challenges require advances in instrumentation. The aim is to have interferometers made of a large number of elements, each one reasonably inexpensive and robust, ensuring easy integration, and smooth operation.

Early digitization and signal processing. As noted above, changes over time of the gain of the receiver electronics is one of the limiting factors in removal of astrophysical foreground power. One promising idea to improve stability is to digitize the analog signal directly at each antenna, rather than remotely, which is the current practice. This early digitization will avoid the use of long analog cables, and analog frequency downconversion. This approach requires stable analog amplifier systems at each antenna and avoidance of RFI generated by the digital electronics. Furthermore, the system clock signal must be distributed precisely to each of the digitizers, moving the instrument phase calibration problem from the analog system into the clock distribution system. Thermal stabilization of the low noise amplifiers (LNAs) at each antenna may be required.

Optical and analog design. The receiver noise temperature is dominated by loss in the antenna as well as the noise in the LNA. HIRAX, for example, has chosen to reduce the system noise by up to 30% by fabricating the LNA directly in the antenna itself, reducing the transmission loss and taking full advantage of low-noise transistors available in these bands.

Antennas for 21 cm experiments range from dipoles for long wavelength experiments to parabolic reflectors, including on-axis dishes as well as cylindrical designs, at shorter wavelengths. Low sidelobes are desirable to allow operation when the Sun is up and to minimize coupling chromatic response into foregrounds. So far, the parabolic reflectors have supported receivers at the focus with struts or tensioned cables, leading to some diffraction and reflections. To illuminate the reflector, they have also included variants of dipole feed antennas with wide beams that have non-negligible cross-talk and frequency-dependence. These choices are typically made to save cost and complexity, but make calibration more difficult. Further studies should include options such as off-axis geometries (like SKA-mid and ngVLA) and possibly horn/Gregorian receivers, keeping marginal costs low while meeting uniformity and bandwidth flatness specifications, and exploring new reflector fabrication techniques. Current instruments are limited by the fact that their interferometric elements are not similar enough and motivate assessment of fabrication tolerances in mass-production.

Calibration. Current instruments rely primarily on sky signals for calibration of the beam and gain. However, this approach has not yet been demonstrated to adequately remove foregrounds with these instruments. The frequency-dependent gain for each input must be known to $\sim 1\%$ on time scales between the integration period ($< 5\,$s scales) and a few hours, depending on the rate of appearance of on-sky radio calibration sources [39]. This challenge can be met by a combination of instrument stability and a suitable calibration scheme. CHIME [62, 63] is updating a classic radio noise-injection scheme which can be used to calibrate many signal chains at once. To implement such an active calibration technique for large arrays will require development of a stable calibration distribution network as well as passive models of gain and beam variation with temperature and dish pointing.

Because the antenna beam pattern (main beam, sidelobes, and polarization) is frequency-dependent, it can mix frequency dependence (related to redshift) and sky location. This problem is expected to be the primary source of contamination from foreground emission into the signal band, and so must be known even more accurately than the electronic gain ($\sim$0.1%) [39]. This level of calibration is difficult for 21 cm telescopes because they are stationary and designed to have large beams for improved survey speed [64]. In addition, some instruments (such as CHIME) have large antennas, which can be difficult to simulate. Many 21 cm instruments are beginning to use signals from small unmanned aerial systems (sUAS, or "drones") and satellites to map the beam shape and measure the gain [65–70]. Ultimately, the beam calibration requirement sets a specification on uniformity in antenna fabrication.

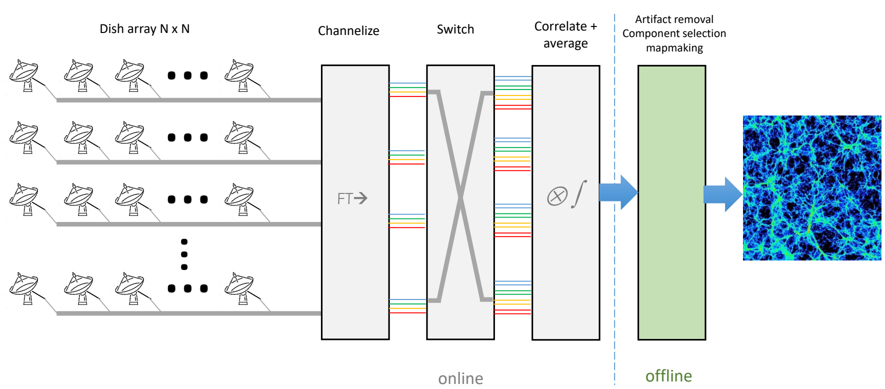

Figure 1: Illustration of anticipated data flow in a large interferometric array. Conversion of waveform data to frequency space, e.g. channelization, is accomplished close to each receiver; coincident data for each frequency bin are collected from all stations through a cross-bar switch (also called a "corner-turn" operation); correlations are constructed for each frequency bin, which can then be time-averaged and stored, followed by physics analysis.

Realtime data flow and processing. Large-N arrays are becoming increasingly software based, particularly when it comes to real-time data compression. Computing requirements for large interferometers come from the correlation burden, real-time calibration, RFI-excision, and the data reduction, transfer, storage, analysis, and synthetic data production (Fig.1). The correlator computation requires development in computing approaches which can improve the cost scaling both for equipment and power. Examples could include using commodity-hosted FPGA's, combined FPGA/CPU systems [71, 72], using/developing dedicated ASIC's [73], or using GPUs to exploit fast-paced hardware updates for correlator computation.

4 Data Analysis Development

Releasing science deliverables for the community from a 21 cm experiment depends crucially on developing an analysis pipeline that can transform vast quantities of data into well characterized frequency maps and power spectra. This is a computationally costly exercise, but does not require continuous real time processing. The analysis challenges center both on the methodology (optimal algorithms have yet to be demonstrated) and software engineering (data volumes are incredibly large). We can divide the analysis up into three broad areas.

Flagging, calibration, and pre-processing at scale. The acquired data are processed to reduce remaining systematic effects. Of particular importance is cleaning of RFI by flagging times and frequency channels that have been contaminated. The problem is well understood within radio astronomy [58], though the effects of residual RFI at the small level of the 21 cm signal is only starting to be addressed [74]. Though much of the calibration must be done in real-time (see above) there are still degrees of freedom that must be corrected in later analysis.

Astrophysical foreground removal. Foreground mitigation falls broadly into two classes: foreground avoidance and foreground cleaning. Foreground avoidance is the simplest of these two approaches, relying on the fact that contamination produced by a typical interferometer configuration is strongest in certain regions of k-space. Producing cosmological results using only the cleanest modes is a simple and effective technique, but it becomes deeply unsatisfactory at low frequencies, particularly in the dark ages. Here Galactic synchrotron and extragalactic point source radiation quickly becomes very bright even at high Galactic latitudes. At the same time, the window of clean modes dramatically narrows due to the relative scaling of the angular diameter distance and Hubble parameter with redshift [75]. Combined, this means that at a given threshold for contamination we exclude increasingly large regions of k-space at high redshifts, significantly degrading any cosmological result.

Foreground cleaning instead of (or in conjunction with) foreground avoidance then becomes an attractive option. These methods rely on detailed knowledge of the instrument response and the sky to predict and subtract the actual foreground signal. The residual contamination is set by both the amplitude of the raw contamination and the accuracy with which the beam has been measured.

Cosmological processing. The next step after foreground cleaning is to compute cosmologically useful quantities such as power spectra and sky maps. This step has been done within the CMB and LSS communities for many years but radio interferometric data brings unique challenges. Nevertheless, conceptual frameworks have been developed to tackle these problems [39, 76, 77]. Several areas of data analysis, then, will require research investment to ensure the success of a large scale 21 cm intensity mapping survey:

1. **Scaling.** A significant challenge is scaling existing analysis techniques to work with the vast increase in expected data in an energy-constrained/post-Moore's Law computing landscape. This process will require optimization of algorithms to reduce the computational cost, and ensuring that the techniques can operate in parallel on leading edge supercomputers.
2. **Systematic robustness.** Both astrophysical uncertainties (such as the exact nature of foregrounds) and instrumental uncertainties (such as calibration and beam optics) cause foreground contamination. Developing more robust cleaning techniques will reduce systematic biases, and

may lead to cost savings by reducing instrumental tolerance requirements.

3. **Improving signal recovery.** The loss of significant numbers of modes during foreground removal reduces our constraining ability generally and particularly affects science that needs access to the largest scales. Foreground removal methods like tidal reconstruction [78, 79] need to be developed that reduce the effect of the 'foreground wedge' [80]. Similarly, traditional reconstruction techniques [81, 82] that recover non-linear modes need to be adapted for the peculiarities of $21\,\mathrm{cm}$ intensity mapping.

5 Simulation needs & challenges

The challenges facing $21\,\mathrm{cm}$ surveys are significant but well understood. However, our ability to tackle them requires sophisticated approaches in instrumental design and offline analysis. It is therefore essential to use simulations to close a feedback loop that allows prediction, and thus refinement, of the effectiveness of a design and analysis strategy. The importance of this testing is especially evident in the face of sophisticated foreground mitigation strategies with the potential for significant signal loss [83]. While expensive to implement, an end-to-end simulation of the entire measurement process is necessary for designing a successful instrument and observational program.

Producing realistic simulations of data from any instrument configuration and propagating these to final cosmological results is a conceptually straightforward prospect:

1. **Produce a suite of full-sky maps of the "true" sky.** These include both the $21\,\mathrm{cm}$ cosmic signal and foregrounds, with one map per frequency bin observed by the instrument.
2. **"Observe" these maps with a simulation pipeline.** This step requires a detailed enough instrument model to provide realistic mock visibility data streams, including effects such as far side lobes, instrumental parameters drift, etc.; and
3. **Feed these mock observations into the data analysis pipeline and produce reduced data cosmological analyses.** This pipeline, discussed Section 4, is the same that would be used on real data. This step requires software tools to compute power spectra ($P(k)/C(\ell, \nu)$) from 3D sky maps or directly from visibilities, or higher order statistics. These tools could then be used to evaluate the realistic performance of different instrument configurations for constraining cosmological models and parameters.

For verification of foreground removal effectiveness, Gaussian or pseudo-Gaussian $21\,\mathrm{cm}$ simulations are largely sufficient [39, 85]. However, for targeting sensitivity to specific effects (e.g. non-Gaussian initial conditions), or in cross-correlation with other probes, more accurate simulations constructed from mock-catalogues will be required. This allows us to produce correctly correlated maps for additional tracers (e.g. LSST photometric galaxies), and also for radio point source contribution to the foregrounds.

Though the relation between HI density and total matter density involves complex environment-dependent processes, simulating it can be done efficiently. Recent work has shown that one can take advantage of the fact that neutral hydrogen in the post-reionization era resides almost entirely inside dark matter halos [84]. Thus, one can calibrate the relation between dark matter halos and HI using hydrodynamic simulations and create $21\,\mathrm{cm}$ maps (Fig. 2) via less expensive methods such as N-body or fast numerical simulations [86–94]. Similarly, while there are large-scale hydrodynamic EoR simulations (e.g. DRAGONS), modelers are parameterizing these numerical methods, and finding efficient ways to constrain those parameters [95].

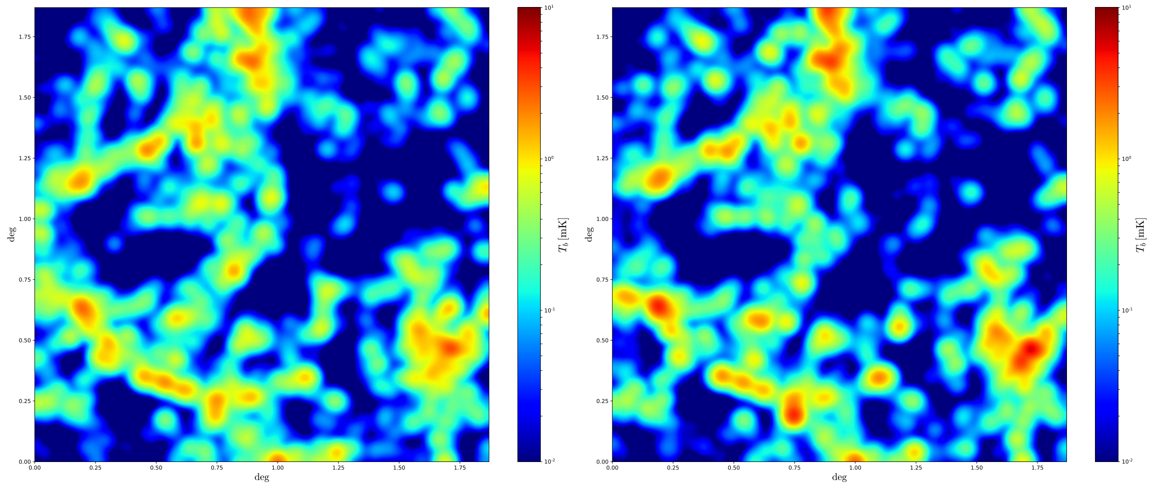

Figure 2: 21 cm maps at a frequency of 710 MHz over a channel width of 1 MHz with an angular resolution of 1.5' over an area of $\simeq 4\ \mathrm{deg}^2$. The map on the left has been created from the state-of-the-art magneto-hydrodynamic simulation IllustrisTNG with a computational cost of $\simeq$18 million cpu hours. The map on the right panel has been generated by assigning HI to dark matter halos of an N-body simulation using the a simplification of the ingredients outlined in [84]. The computational cost of the N-body simulation is much lower than that of the full hydrodynamical simulation, and allows modelling of the HI field in a very precise and robust manner. The shapes of the power spectra of these two simulations differ by only $\sim 5\%$ from the largest scales down to $k = 1\mathrm{h\ Mpc}^{-1}$.

Galactic synchrotron is the largest foreground contaminant and simulations must ensure they are not artificially easy to clean. A simple approximation can be produced by proceeding from a full sky map at a radio frequency and scaling to different frequencies based on the known spectral index of Galactic synchrotron radiation. However this is not sufficient at the dynamic range between the foregrounds and the $21\,$cm signal and one must be careful to include: spectral variations about a pure power law; small scale angular fluctuations not captured in existing surveys; and polarization, including the effects of emission at a wide range of Faraday depths which generates significant spectral structure in the polarized emission [39]. More sophisticated Galactic models, for example from MHD simulations, could also be developed and used here. Additional observations with existing instruments will better characterize the spectral behavior of the foregrounds.

In Step 2, a realistic instrument simulation pipeline would take the maps discussed and convolve them with the complex beam for each antenna in the interferometer [96]. This can be done by direct convolution utilizing the fact that for a transit telescope it is sufficient to generate a single day of data. However, for wide-field transit interferometers this can be performed more efficiently in harmonic space using the m-mode formalism [40] ($O(N \log N)$ instead of $O(N^2)$). Some of the required code would be similar to code used in CMB science, such as the TOAST package using fast numerical techniques for beam convolution [97].

These simulations require realistic models of the telescope beams. Electromagnetic simulation codes such as CST, GRASP and HFSS can be used for this, but achieving the accuracy required is challenging computationally [98–100]. A complementary approach is to generate synthetic beams with sufficient complexity to capture the challenges posed by real beams. These are computationally easier to produce, but must be informed by real measurements and electromagnetic simulations to ensure their realism, and may be aided by machine learning algorithms.

Capturing non-idealities in the analog system, particularly gain variations, is mostly straightforward as these can be applied directly to the ideal timestreams. Additionally, one needs to include

Name	Optimized	Steerable	Type	Elements	Redshift	First light
Existing w/ data:						
GMRT [101]	N	Y	interferometer	30 dual-pol × 45 m dishes	28	1995
GBT [102]	N	Y	single dish	1 dual-pol on 100 m dish	∼0.8	2009
Dedicated exp'ts:						
OVRO-LWA [103, 104]	Y	N	interferometer	288 dual-pol dipoles	16 – 52	2012
MWA [105, 106]	Y	electronic	interferometer	256 tiles of 16 dual-pol dipoles	3.7–16	2013
PAPER [107, 108]	Y	N	interferometer	128 dual-pol dipole/reflector	7–12	2010
HERA [109, 110]	Y	N	interferometer	350 dual-pol 14 m dish (staged deploy't)	6–30	2016
LOFAR [111, 112]	Y	electronic	interferometer	3400 tiles of 16 dual-pol dipoles	5–11	2007
				4224 dual-pol dipoles	17–141	
CHIME [113, 114]	Y	N	cylinder interferometer	1024 dual-pol over 4 cyl	0.75 – 2.5	2017
HIRAX [115, 116]	Y	limited	dish interferometer	1024 dual-pol × 6 m dishes	0.75 – 2.5	2020
Tianlai Dish [117, 118]	Y	Y	dish interferometer	16 dual-pol × 6 m dishes	0 – 1.5	2016
Tianlai Cylinder [117, 118]	Y	N	cylinder interferometer	96 dual-pol over 3 cyl	0 – 1.5	2016
OWFA [119, 120]	N	Y	cylinder interferometer	264 single-pol	$\sim 3.4\pm0.3$	2019
BINGO [121, 122]	Y	N	single dish	∼60 dual-pol sharing ∼50 m dish	0.12 – 0.45	2020
Dedicated R&D:						
BMX	Y	N	dish interferometer	4 dual-pol ×4 m off-axis dishes	0 – 0.3	2017
NCLE [123]	Y	N	satellite	3×5 m monopole ant. at Earth-Moon L_2	> 17	2018
PAON-4 [124, 125]	Y	limited	dish interferometer	4 dual-pol ×5 m dishes	0 – 0.14	2015
Non-dedicated:						
MeerKAT	N	Y	single-sish	64 dual-pol × 13.5 m dishes	0 – 1.4	2016
SKA1-MID	N	Y	single-dish	∼ 200 dual-pol × ∼ 15 m dishes	0 – 3	2028
SKA1-LOW [126]	N	electronic	interferometer	269,312 dual-pol dipoles	3–27	2028
Proposed:						
PUMA [26, 127]	Y	limited	dish interferometer	5000, 32000 or 64000 dual-pol × 6 m dishes	0.3 – 6	<2030

Table 1: Current and planned 21 cm intensity mapping experiments. The "First light" column refers to first light for 21 cm observations for non-dedicated experiments. In the "Optimized" column, we note whether the telescope has been designed with intensity mapping as its primary scientific goal. For MeerKAT and SKA-MID, dishes will likely be used in a single-dish mode, with interferometric capability used only for gain calibration.

time-dependent beam convolution (including position and brightness) for temporally varying sources such as solar, jovian and lunar emission as well as the effects of RFI at low levels [74]. Including calibration uncertainties poses a particular challenge, because of the realtime calibration and compression of the instrument. Simulating these effects requires either: generating data at the full uncompressed rate, applying gain variations, and then performing the calibration and compression processes; or the computationally easier alternative of generating models of the effective calibration uncertainties.

After the first two stages, mock observations are then fed to the proposed data analysis pipeline, and propagated through to final cosmological products, to assess analysis systematics, instrument design, real-time calibration, etc. to determine whether the pipeline is sufficient to meet the science goals. Though the simulation program is well defined, there are many open challenges to address:

1. **Understanding the HI Distribution.** To map the HI distribution to the cosmologically useful matter distribution requires cutting edge hydrodynamic simulations to capture the small halos that HI favours over a cosmologically interesting volume.
2. **Scale.** We need to be able to produce large numbers of emulators that Monte-Carlo over the experimental uncertainties.
3. **Improving the feedback loop.** While a straightforward version of the simulation loop above can tell us whether a proposed design meets requirements, it does not show how to improve the design to ensure that it does. For a complex instrument with many design parameters it is essential to be able to guide this process to find the most relevant combinations of changes.

6 Participation in Current and Near-term (Stage I) Programs

Support for both small dedicated test-bed instruments and participation in existing and future large-scale initiatives, both US-led and international, will enable development and testing of the methods presented above and will benefit 21 cm intensity mapping efforts ranging from the Dark Ages to the post-EoR epoch. We believe that with rather modest investment of resources, such R&D will enable current experiments to extract maximum science while paving the way for future and even more exciting telescopes (Table 1). In particular, these efforts are the only way to make progress in foreground removal, instrument calibration, correlating signals from large arrays, dealing with RFI, achieving adequate sensitivity, and analyzing huge data cubes.

While there has been considerable funding from the US for Cosmic Dawn/EoR programs, currently there is no significant US funding for any of the existing post-EoR Stage I programs (CHIME, HIRAX, Tianlai). Post-EoR 21 cm intensity mapping is an unexploited probe of dark energy and inflation that is complementary to CMB and optical surveys. Participation in these efforts, or a new effort, would enable a coherent development plan that would include:

1. Construction of a test bed with 10-100 interferometer elements to test technologies (antennas and electronic as well as internal calibration systems).
2. Construction of a large, ~ 1000 element array to understand specific problems of operating such an array, including calibration and stability issues. Such an array should be operated with a (pairwise) correlator system first.
3. Development of an FFT beamformer and associated real-time calibration for this array.
4. Construction of a Stage II array with $10^4 - 10^5$ elements. An instrument of this scale is necessary to survey the entire post-EoR epoch.

Hardware development is not enough. An increasingly large share of the budget for all 21 cm intensity mapping programs is in the development of production- or system-level software. We need to pay close attention to developing software that does the real-time analysis (calibration, RFI excision, etc.), integrate it into a system, and fully test it.

7 Conclusion

A wide range of Astro2020 science goals depend on the success of 21 cm intensity mapping for measuring large scale structure in the universe over enormously larger volumes than possible today. This white paper has described a plan to advance this technique over the next decade and includes 1) development and testing of key technologies for reliable, robust single antenna systems which could be assembled as transit interferometric arrays, and associated central real time control/acquisition and computing systems. Most subsystems would be common to Cosmic Dawn/EoR and post-EoR observations. It also includes development of software for 2) data analysis and 3) simulations to realistically evaluate different instrument configurations. A significant fraction of the software tools would be common to all epochs. These technical achievements require 4) support for participation in current (Stage I) experiments to lay the groundwork for next generation (Stage II) experiments. As described above, Stage I experiments have already taught many lessons which must be understood before embarking on the next generation.

References

[1] Jordan Mirocha, Daniel Jacobs, Josh Dillon, Steve Furlanetto, Jonathan Pober, Adrian Liu, James Aguirre, Yacine Ali-Haïmoud, Marcelo Alvarez, Adam Beardsley, George Becker, Judd Bowman, Patrick Breysse, Volker Bromm, Jack Burns, Xuelei Chen, Tzu-Ching Chang, Hsin Chiang, Joanne Cohn, David DeBoer, Cora Dvorkin, Anastasia Fialkov, Nick Gnedin, Bryna Hazelton, Masui Kiyoshi, Saul Kohn, Leon Koopmans, Ely Kovetz, Paul La Plante, Adam Lidz, Yin-Zhe Ma, Yi Mao, Andrei Mesinger, Julian Muñoz, Steven Murray, Aaron Parsons, Jonathan Pritchard, Jonathan Sievers, Eric Switzer, Nithyanand an Thyagarajan, Eli Visbal, and Matias Zaldarriaga. Astro2020 Science White Paper: First Stars and Black Holes at Cosmic Dawn with Redshifted 21-cm Observations. arXiv e-prints, page arXiv:1903.06218, Mar 2019.

[2] Steven Furlanetto, Judd D. Bowman, Jordan Mirocha, Jonathan C. Pober, Jack Burns, Chris L. Carilli, Julian Munoz, James Aguirre, Yacine Ali-Haimoud, Marcelo Alvarez, Adam Beardsley, George Becker, Patrick Breysse, Volker Bromm, Philip Bull, Tzu-Ching Chang, Xuelei Chen, Hsin Chiang, Joanne Cohn, Frederick Davies, David DeBoer, Joshua Dillon, Olivier Doré, Cora Dvorkin, Anastasia Fialkov, Bryna Hazelton, Daniel Jacobs, Kirit Karkare, Saul Kohn, Leon Koopmans, Ely Kovetz, Paul La Plante, Adam Lidz, Adrian Liu, Yin-Zhe Ma, Yi Mao, Kiyoshi Masui, Andrew Mesinger, Steven Murray, Aaron Parsons, Benjamin Saliwanchik, Jonathan Sievers, Nithyanandan Thyagarajan, Hy Trac, Eli Visbal, and Matias Zaldarriaga. Astro 2020 Science White Paper: Fundamental Cosmology in the Dark Ages with 21-cm Line Fluctuations. arXiv e-prints, page arXiv:1903.06212, Mar 2019.

[3] Steven Furlanetto, Chris L. Carilli, Jordan Mirocha, James Aguirre, Yacine Ali-Haimoud, Marcelo Alvarez, Adam Beardsley, George Becker, Judd D. Bowman, Patrick Breysse, Volker Bromm, Philip Bull, Jack Burns, Isabella P. Carucci, Tzu-Ching Chang, Xuelei Chen, Hsin Chiang, Joanne Cohn, Frederick Davies, David DeBoer, Joshua Dillon, Olivier Doré, Cora Dvorkin, Anastasia Fialkov, Nick Gnedin, Bryna Hazelton, Daniel Jacobs, Kirit Karkare, Saul Kohn, Leon Koopmans, Ely Kovetz, Paul La Plante, Adam Lidz, Adrian Liu, Yin-Zhe Ma, Yi Mao, Kiyoshi Masui, Matthew McQuinn, Andrei Mesinger, Julian Munoz, Steven Murray, Aaron Parsons, Jonathan Pober, Benjamin Saliwanchik, Jonathan Sievers, Eric Switzer, Nithyanandan Thyagarajan, Hy Trac, Eli Visbal, and Matias Zaldarriaga. Astro2020 Science White Paper: Insights Into the Epoch of Reionization with the Highly-Redshifted 21-cm Line. arXiv e-prints, page arXiv:1903.06204, Mar 2019.

[4] Steven Furlanetto, Adam Beardsley, Chris L. Carilli, Jordan Mirocha, James Aguirre, Yacine Ali-Haimoud, Marcelo Alvarez, George Becker, Judd D. Bowman, Patrick Breysse, Volker Bromm, Philip Bull, Jack Burns, Isabella P. Carucci, Tzu-Ching Chang, Hsin Chiang, Joanne Cohn, Frederick Davies, David DeBoer, Mark Dickinson, Joshua Dillon, Olivier Doré, Cora Dvorkin, Anastasia Fialkov, Steven Finkelstein, Nick Gnedin, Bryna Hazelton, Daniel Jacobs, Kirit Karkare, Leon Koopmans, Ely Kovetz, Paul La Plante, Adam Lidz, Adrian Liu, Yin-Zhe Ma, Yi Mao, Kiyoshi Masui, Matthew McQuinn, Andrei Mesinger, Julian Munoz, Steven Murray, Aaron Parsons, Jonathan Pober, Brant Robertson, Jonathan Sievers, Eric Switzer, Nithyanandan Thyagarajan, Hy Trac, Eli Visbal, and Matias Zaldarriaga. Astro2020 Science White Paper: Synergies Between Galaxy Surveys and Reionization Measurements. arXiv e-prints, page arXiv:1903.06197, Mar 2019.

[5] Anne Hutter, Pratika Dayal, Sangeeta Malhotra, James Rhoads, Tirthankar Roy Choudhury, Benedetta Ciardi, Christopher J. Conselice, Asantha Cooray, Jean-Gabriel Cuby, Kanan K. Datta, Xiaohui Fan, Steven Finkelstein, Christopher Hirata, Ilian Iliev, Rolf Jansen, Koki Kakiichi, Anton Koekemoer, Umberto Maio, Suman Majumdar, Garrelt Mellema, Rajesh Mondal, Casey Papovich, Jason Rhodes, Martin Sahlén, Anna Schauer, Keitaro Takahashi, Graziano Ucci, Rogier Windhorst, and Erik Zackrisson. Astro2020 Science White Paper: A proposal to exploit galaxy-21cm synergies to shed light on the Epoch of Reionization. arXiv e-prints, page arXiv:1903.03628, Mar 2019.

[6] Tzu-Ching Chang, Angus Beane, Olivier Dore, Adam Lidz, Lluis Mas-Ribas, Guochao Sun, Marcelo Alvarez, Ritoban Basu Thakur, Philippe Berger, Matthieu Bethermin, Jamie Bock, Charles M. Bradford, Patrick Breysse, Denis Burgarella, Vassilis Charmand aris, Yun-Ting Cheng, Kieran Cleary, Asantha Cooray, Abigail Crites, Aaron Ewall-Wice, Xiaohui Fan, Steve Finkelstein, Steve Furlanetto, Jacqueline Hewitt, Jonathon Hunacek, Phil Korngut, Ely Kovetz, Gregg Hallinan, Caroline Heneka, Guilaine Lagache, Charles Lawrence, Joseph Lazio, Adrian Liu, Dan Marrone, Aaron Parsons, Anthony Readhead, Jason Rhodes, Dominik Riechers, Michael Seiffert, Gordon Stacey, Eli Visbal, Hao-Yi Wu, Michael Zemcov, and Zheng Zheng. Tomography of the Cosmic Dawn and Reionization Eras with Multiple Tracers. arXiv e-prints, page arXiv:1903.11744, Mar 2019.

[7] Marcelo A. Alvarez, Anastasia Fialkov, Paul La Plante, James Aguirre, Yacine Ali-Haïmoud, George Becker, Judd Bowman, Patrick Breysse, Volker Bromm, Philip Bull, Jack Burns, Nico Cappelluti, Isabella Carucci, Tzu-Ching Chang, Kieran Cleary, Asantha Cooray, Xuelei Chen, Hsin Chiang, Joanne Cohn, David DeBoer, Joshua Dillon, Olivier Doré, Cora Dvorkin, Simone Ferraro, Steven Furlanetto, Bryna Hazelton, J. Colin Hill, Daniel Jacobs, Kirit Karkare, Garrett K. Keating, Léon Koopmans, Ely Kovetz, Adam Lidz, Adrian Liu, Yin-Zhe Ma, Yi Mao, Kiyoshi Masui, Matthew McQuinn, Jordan Mirocha, Julian Muñoz, Steven Murray, Aaron Parsons, Jonathan Pober, Benjamin Saliwanchik, Jonathan Sievers, Nithyanandan Thyagarajan, Hy Trac, Alexey Vikhlinin, Eli Visbal, and Matias Zaldarriaga. Mapping Cosmic Dawn and Reionization: Challenges and Synergies. arXiv e-prints, page arXiv:1903.04580, Mar 2019.

[8] Asantha Cooray, James Aguirre, Yacine Ali-Haimoud, Marcelo Alvarez, Phil Appleton, Lee Armus, George Becker, Jamie Bock, Rebecca Bowler, Judd Bowman, Matt Bradford, Patrick Breysse, Volker Bromm, Jack Burns, Karina Caputi, Marco Castellano, Tzu-Ching Chang, Ranga Chary, Hsin Chiang, Joanne Cohn, Chris Conselice, Jean-Gabriel Cuby, Frederick Davies, Pratika Dayal, Olivier Dore, Duncan Farrah, Andrea Ferrara, Steven Finkelstein, Steven Furlanetto, Bryna Hazelton, Caroline Heneka, Anne Hutter, Daniel Jacobs, Leon Koopmans, Ely Kovetz, Paul La Piante, Olivier Le Fevre, Adrian Liu, Jingzhe Ma, Yin-Zhe Ma, Sangeeta Malhotra, Yi Mao, Dan Marrone, Kiyoshi Masui, Matthew McQuinn, Jordan Mirocha, Daniel Mortlock, Eric Murphy, Hooshang Nayyeri, Priya Natarajan, Thyagarajan Nithyanand an, Aaron Parsons, Roser Pello, Alexandra Pope, James Rhoads, Jason Rhodes, Dominik Riechers, Brant Robertson, Claudia Scarlata, Stephen Serjeant, Benjamin Saliwanchik, Ruben Salvaterra, Rafffaella Schneider, Marta Silva, Martin Sahlén, Mario G. Santos, Eric Switzer, Pasquale Temi, Hy Trac, Aparna Venkatesan, Eli Visbal, Matias Zaldarriaga, Michael Zemcov, and Zheng Zheng. Cosmic Dawn and Reionization: Astrophysics in the Final Frontier. arXiv e-prints, page arXiv:1903.03629, Mar 2019.

[9] Ely D. Kovetz, Patrick C. Breysse, Adam Lidz, Jamie Bock, Charles M. Bradford, Tzu-Ching Chang, Simon Foreman, Hamsa Padmanabhan, Anthony Pullen, Dominik Riechers, Marta B. Silva, and Eric Switzer. Astrophysics and Cosmology with Line-Intensity Mapping. arXiv e-prints, page arXiv:1903.04496, Mar 2019.

[10] Adrian Liu, James Aguirre, Yacine Ali-Haimoud, Marcelo Alvarez, Adam Beardsley, George Becker, Judd Bowman, Patrick Breysse, Volker Bromm, Philip Bull, Jack Burns, Isabella P. Carucci, Tzu-Ching Chang, Xuelei Chen, Hsin Chiang, Joanne Cohn, David DeBoer, Joshua Dillon, Olivier Doré, Cora Dvorkin, Anastasia Fialkov, Steven Furlanetto, Nick Gnedin, Bryna Hazelton, Jacqueline Hewitt, Daniel Jacobs, Kirit Karkare, Marc Klein Wolt, Saul Kohn, Leon Koopmans, Ely Kovetz, Paul La Plante, Adam Lidz, Yin-Zhe Ma, Yi Mao, Kiyoshi Masui, Andrei Mesinger, Jordan Mirocha, Julian Munoz, Steven Murray, Laura Newburgh, Aaron Parsons, Jonathan Pober, Jonathan Pritchard, Benjamin Saliwanchik, Jonathan Sievers, Nithyanandan Thyagarajan, Hy Trac, Eli Visbal, and Matias Zaldarriaga. Cosmology with the Highly Redshifted 21cm Line. arXiv e-prints, page arXiv:1903.06240, Mar 2019.

[11] P. Daniel Meerburg, Daniel Green, Muntazir Abidi, Mustafa A. Amin, Peter Adshead, Zeeshan Ahmed, David Alonso, Behzad Ansarinejad, Robert Armstrong, Santiago Avila, Carlo Baccigalupi, Tobias Baldauf, Mario Ballardini, Kevin Bandura, Nicola Bartolo, Nicholas Battaglia, Daniel Baumann, Chetan Bavdhankar, José Luis Bernal, Florian Beutler, Matteo Biagetti, Colin Bischoff, Jonathan Blazek, J. Richard Bond, Julian Borrill, François R. Bouchet, Philip Bull, Cliff Burgess, Christian Byrnes, Erminia Calabrese, John E. Carlstrom, Emanuele Castorina, Anthony Challinor, Tzu-Ching Chang, Jonas Chaves-Montero, Xingang Chen, Christophe Yeche, Asantha Cooray, William Coulton, Thomas Crawford, Elisa Chisari, Francis-Yan Cyr-Racine, Guido D'Amico, Paolo de Bernardis, Axel de la Macorra, Olivier Doré, Adri Duivenvoorden, Joanna Dunkley, Cora Dvorkin, Alexander Eggemeier, Stephanie Escoffier, Tom Essinger-Hileman, Matteo Fasiello, Simone Ferraro, Raphael Flauger, Andreu Font-Ribera, Simon Foreman, Oliver Friedrich, Juan Garcia-Bellido, Martina Gerbino, Vera Gluscevic, Garrett Goon, Krzysztof M. Gorski, Jon E. Gudmundsson, Nikhel Gupta, Shaul Hanany, Will Hand ley, Adam J. Hawken, J. Colin Hill, Christopher M. Hirata, Renée Hložek, Gilbert Holder, Dragan Huterer, Marc Kamionkowski, Kirit S. Karkare, Ryan E. Keeley, William Kinney, Theodore Kisner, Jean-Paul Kneib, Lloyd Knox, Savvas M. Koushiappas, Ely D. Kovetz, Kazuya Koyama, Benjamin L'Huillier, Ofer Lahav, Massimiliano Lattanzi, Hayden Lee, Michele Liguori, Marilena Loverde, Mathew Madhavacheril, Juan Maldacena, M. C. David Marsh, Kiyoshi Masui, Sabino Matarrese, Liam McAllister, Jeff McMahon, Matthew McQuinn, Joel Meyers, Mehrdad Mirbabayi, Azadeh Moradinezhad Dizgah, Pavel Motloch, Suvodip Mukherjee, Julian B. Muñoz, Adam D. Myers, Johanna Nagy, Pavel Naselsky, Federico Nati, Newburgh, Alberto Nicolis, Michael D. Niemack, Gustavo Niz, Andrei Nomerotski, Lyman Page, Enrico Pajer, Hamsa Padmanabhan, Gonzalo A. Palma, Hiranya V. Peiris, Will J. Percival, Francesco Piacentni, Guilherme L. Pimentel, Levon Pogosian, Chanda Prescod-Weinstein, Clement Pryke, Giuseppe Puglisi, Benjamin Racine, Radek Stompor, Marco Raveri, Mathieu Remazeilles, Gracca Rocha, Ashley J. Ross, Graziano Rossi, John Ruhl, Misao Sasaki, Emmanuel Schaan, Alessandro Schillaci, Marcel Schmittfull, Neelima Sehgal, Leonardo Senatore, Hee-Jong Seo, Huanyuan Shan, Sarah Shandera, Blake D. Sherwin, Eva Silverstein, Sara Simon, Anže Slosar, Suzanne Staggs, Glenn Starkman, Albert Stebbins, Aritoki Suzuki, Eric R. Switzer, Peter Timbie, Andrew J. Tolley, Maurizio Tomasi, Matthieu Tristram, Mark Trodden, Yu-Dai Tsai, Cora Uhlemann, Caterina Umilta, Alexander van Engelen, M. Vargas-Magaña,

Abigail Vieregg, Benjamin Wallisch, David Wands, Benjamin Wandelt, Yi Wang, Scott Watson, Mark Wise, W. L. K. Wu, Zhong-Zhi Xianyu, Weishuang Xu, Siavash Yasini, Sam Young, Duan Yutong, Matias Zaldarriaga, Michael Zemcov, Gong-Bo Zhao, Yi Zheng, and Ningfeng Zhu. Primordial Non-Gaussianity. arXiv e-prints, page arXiv:1903.04409, Mar 2019.

[12] Anže Slosar, Xingang Chen, Cora Dvorkin, Daniel Green, P. Daniel Meerburg, Eva Silverstein, and Benjamin Wallisch. Scratches from the Past: Inflationary Archaeology through Features in the Power Spectrum of Primordial Fluctuations. arXiv e-prints, page arXiv:1903.09883, Mar 2019.

[13] Anže Slosar, Tamara Davis, Daniel Eisenstein, Renée Hložek, Mustapha Ishak-Boushaki, Rachel Mand elbaum, Phil Marshall, Jeremy Sakstein, and Martin White. Dark Energy and Modified Gravity. arXiv e-prints, page arXiv:1903.12016, Mar 2019.

[14] Cora Dvorkin, Martina Gerbino, David Alonso, Nicholas Battaglia, Simeon Bird, Ana Diaz Rivero, Andreu Font-Ribera, George Fuller, Massimiliano Lattanzi, Marilena Loverde, Julian B. Muñoz, Blake Sherwin, Anže Slosar, and Francisco Villaescusa-Navarro. Neutrino Mass from Cosmology: Probing Physics Beyond the Standard Model. arXiv e-prints, page arXiv:1903.03689, Mar 2019.

[15] Ryan Lynch, Paul Brook, Shami Chatterjee, Timoth Dolch, Michael Kramer, Michael T. Lam, Natalia Lewand owska, Maura McLaughlin, Nihan Pol, and Ingrid Stairs. The Virtues of Time and Cadence for Pulsars and Fast Transients. In BAAS, volume 51, page 461, May 2019.

[16] Vikram Ravi, Nicholas Battaglia, Sarah Burke-Spolaor, Shami Chatterjee, James Cordes, Gregg Hallinan, Casey Law, T. Joseph W. Lazio, Kiyoshi Masui, and Matthew McQuinn. Fast Radio Burst Tomography of the Unseen Universe. In BAAS, volume 51, page 420, May 2019.

[17] Casey Law, Ben Margalit, Nipuni T. Palliyaguru, Brian D. Metzger, Lorenzo Sironi, Yong Zheng, Edo Berger, Raffaella Margutti, Andrei Beloborodov, and Matt Nicholl. Radio Time-Domain Signatures of Magnetar Birth. In BAAS, volume 51, page 319, May 2019.

[18] Luke Kelley, M. Charisi, S. Burke-Spolaor, J. Simon, L. Blecha, T. Bogdanovic, M. Colpi, J. Comerford, D. D'Orazio, and M. Dotti. Multi-Messenger Astrophysics With Pulsar Timing Arrays. In BAAS, volume 51, page 490, May 2019.

[19] Stephen Taylor, Sarah Burke-Spolaor, Paul T. Baker, Maria Charisi, Kristina Islo, Luke Z. Kelley, Dustin R. Madison, Joseph Simon, Sarah Vigeland, and Nanograv Collaboration. Supermassive Black-hole Demographics &Environments With Pulsar Timing Arrays. In BAAS, volume 51, page 336, May 2019.

[20] James Cordes, Maura A. McLaughlin, and Nanograv Collaboration. Gravitational Waves, Extreme Astrophysics, and Fundamental Physics with Precision Pulsar Timing. In BAAS, volume 51, page 447, May 2019.

[21] Xavier Siemens, Jeffrey Hazboun, Paul T. Baker, Sarah Burke-Spolaor, Dustin R. Madison, Chiara Mingarelli, Joseph Simon, and Tristan Smith. Physics Beyond the Standard Model With Pulsar Timing Arrays. In BAAS, volume 51, page 437, May 2019.

[22] Emmanuel Fonseca, Paul Demorest, Scott Ransom, and Ingrid Stairs. Fundamental Physics with Radio Millisecond Pulsars. In BAAS, volume 51, page 425, May 2019.

[23] Duncan Lorimer, Nihan Pol, Kaustubh Rajwade, Kshitij Aggarwal, Devansh Agarwal, Jay Strader, Natalia Lewand owska, David Kaplan, Tyler Cohen, and Paul Demorest. Radio Pulsar Populations. In BAAS, volume 51, page 261, May 2019.

[24] J. D. Bowman, A. E. E. Rogers, R. A. Monsalve, T. J. Mozdzen, and N. Mahesh. An absorption profile centred at 78 megahertz in the sky-averaged spectrum. Nature, 555:67–70, March 2018.

[25] Adrian Liu, Jonathan R. Pritchard, Rupert Allison, Aaron R. Parsons, Uroš Seljak, and Blake D. Sherwin. Eliminating the optical depth nuisance from the CMB with 21 cm cosmology. Phys. Rev. D, 93(4):043013, Feb 2016.

[26] Anže Slosar. Packed ultra-wideband mapping array (puma): A radio telescope for cosmology and transients. Submission to Astrophysics and Astronomy Decadal Survey, Jul 2019.

[27] CHIME/FRB Collaboration, M. Amiri, K. Bandura, M. Bhardwaj, P. Boubel, M. M. Boyce, P. J. Boyle, C. Brar, M. Burhanpurkar, and P. Chawla. Observations of fast radio bursts at frequencies down to 400 megahertz. Nature, 566(7743):230–234, Jan 2019.

[28] The Hydrogen Epoch of Reionization Array (HERA) Collaboration. A roadmap for astrophysics and cosmology with high-redshift 21 cm intensity mapping. Submission to Astrophysics and Astronomy Decadal Survey, Jul 2019.

[29] Zaki S. Ali, Aaron R. Parsons, Haoxuan Zheng, Jonathan C. Pober, Adrian Liu, James E. Aguirre, Richard F. Bradley, Gianni Bernardi, Chris L. Carilli, Carina Cheng, David R. DeBoer, Matthew R. Dexter, Jasper Grobbelaar, Jasper Horrell, Daniel C. Jacobs, Pat Klima, David H. E. MacMahon, Matthys Maree, David F. Moore, Nima Razavi, Irina I. Stefan, William P. Walbrugh, and Andre Walker. PAPER-64 Constraints on Reionization: The 21 cm Power Spectrum at z = 8.4. ApJ, 809(1):61, Aug 2015.

[30] Zaki S. Ali, Aaron R. Parsons, Haoxuan Zheng, Jonathan C. Pober, Adrian Liu, James E. Aguirre, Richard F. Bradley, Gianni Bernardi, Chris L. Carilli, Carina Cheng, David R. DeBoer, Matthew R. Dexter, Jasper Grobbelaar, Jasper Horrell, Daniel C. Jacobs, Pat Klima, David H. E. MacMahon, Matthys Maree, David F. Moore, Nima Razavi, Irina I. Stefan, William P. Walbrugh, and Andre Walker. Erratum: "PAPER-64 Constraints on Reionization: The 21 cm Power Spectrum at z = 8.4" (¡A href="http://doi.org/10.1088/0004-637x/809/1/61"¿2015, ApJ, 809, 61¡/A¿). ApJ, 863(2):201, Aug 2018.

[31] T.-C. Chang, U.-L. Pen, K. Bandura, and J. B. Peterson. An intensity map of hydrogen 21-cm emission at redshift z˜0.8. Nature, 466:463–465, July 2010.

[32] K. W. Masui, E. R. Switzer, N. Banavar, K. Bandura, C. Blake, L.-M. Calin, T.-C. Chang, X. Chen, Y.-C. Li, Y.-W. Liao, A. Natarajan, U.-L. Pen, J. B. Peterson, J. R. Shaw, and T. C. Voytek. Measurement of 21 cm Brightness Fluctuations at z ˜ 0.8 in Cross-correlation. ApJ, 763:L20, January 2013.

[33] E. R. Switzer, K. W. Masui, K. Bandura, L.-M. Calin, T.-C. Chang, X.-L. Chen, Y.-C. Li, Y.-W. Liao, A. Natarajan, U.-L. Pen, J. B. Peterson, J. R. Shaw, and T. C. Voytek. Determination of z 0.8 neutral hydrogen fluctuations using the 21 cm intensity mapping autocorrelation. MNRAS, 434:L46–L50, July 2013.

[34] C. J. Anderson, N. J. Luciw, Y. C. Li, C. Y. Kuo, J. Yadav, K. W. Masui, T. C. Chang, X. Chen, N. Oppermann, Y. W. Liao, U. L. Pen, D. C. Price, L. Staveley-Smith, E. R. Switzer, P. T. Timbie, and L. Wolz. Low-amplitude clustering in low-redshift 21-cm intensity maps cross-correlated with 2dF galaxy densities. MNRAS, 476(3):3382–3392, May 2018.

[35] P. Procopio, R. B. Wayth, J. Line, C. M. Trott, H. T. Intema, D. A. Mitchell, B. Pindor, J. Riding, S. J. Tingay, M. E. Bell, J. R. Callingham, K. S. Dwarakanath, B.-Q. For, B. M. Gaensler, P. J. Hancock, L. Hindson, N. Hurley-Walker, M. Johnston-Hollitt, A. D. Kapińska, E. Lenc, B. McKinley, J. Morgan, A. Offringa, L. Staveley-Smith, C. Wu, and Q. Zheng. A High-Resolution Foreground Model for the MWA EoR1 Field: Model and Implications for EoR Power Spectrum Analysis. PASA, 34:e033, August 2017.

[36] J. C. Pober, A. R. Parsons, J. E. Aguirre, Z. Ali, R. F. Bradley, C. L. Carilli, D. DeBoer, M. Dexter, N. E. Gugliucci, D. C. Jacobs, P. J. Klima, D. MacMahon, J. Manley, D. F. Moore, I. I. Stefan, and W. P. Walbrugh. Opening the 21 cm Epoch of Reionization Window: Measurements of Foreground Isolation with PAPER. ApJ, 768:L36, May 2013.

[37] H.-J. Seo and C. M. Hirata. The foreground wedge and 21-cm BAO surveys. MNRAS, 456:3142–3156, March 2016.

[38] A. Liu and M. Tegmark. How well can we measure and understand foregrounds with 21-cm experiments? MNRAS, 419:3491–3504, February 2012.

[39] J Richard Shaw, Kris Sigurdson, Michael Sitwell, Albert Stebbins, and Ue-Li Pen. Coaxing Cosmic 21cm Fluctuations from the Polarized Sky using m-mode Analysis. arXiv.org, January 2014a.

[40] J Richard Shaw, Kris Sigurdson, Ue-Li Pen, Albert Stebbins, and Michael Sitwell. All-Sky Interferometry with Spherical Harmonic Transit Telescopes. arXiv.org, February 2013.

[41] R. Ansari, J. E. Campagne, P. Colom, J. M. Le Goff, C. Magneville, J. M. Martin, M. Moniez, J. Rich, and C. Yèche. 21 cm observation of large-scale structures at z ~1. Instrument sensitivity and foreground subtraction. A&A, 540:A129, Apr 2012.

[42] James Kent, Jayce Dowell, Adam Beardsley, Nithyanandan Thyagarajan, Greg Taylor, and Judd Bowman. A real-time, all-sky, high time resolution, direct imager for the long wavelength array. MNRAS, 486(4):5052–5060, Jul 2019.

[43] U.-L. Pen. Gravitational lensing of epoch-of-reionization gas. New A, 9:417–424, July 2004.

[44] M. Tegmark and M. Zaldarriaga. Fast Fourier transform telescope. Phys. Rev. D, 79(8):083530–+, April 2009.

[45] M. Tegmark and M. Zaldarriaga. Omniscopes: Large area telescope arrays with only Nlog(N) computational cost. Phys. Rev. D, 82(10):103501, November 2010.

[46] K. W. Masui, J. R. Shaw, C. Ng, K. M. Smith, K. Vanderlinde, and A. Paradise. Algorithms for FFT Beamforming Radio Interferometers. ArXiv e-prints, October 2017.

[47] G. Foster, J. Hickish, A. Magro, D. Price, and K. Zarb Adami. Implementation of a direct-imaging and FX correlator for the BEST-2 array. MNRAS, 439(3):3180–3188, Apr 2014.

[48] Adam P. Beardsley, Nithyanandan Thyagarajan, Judd D. Bowman, and Miguel F. Morales. An efficient feedback calibration algorithm for direct imaging radio telescopes. MNRAS, 470(4):4720–4731, Oct 2017.

[49] A. Liu, M. Tegmark, S. Morrison, A. Lutomirski, and M. Zaldarriaga. Precision calibration of radio interferometers using redundant baselines. MNRAS, 408:1029–1050, October 2010.

[50] C. L. Carilli, B. Nikolic, N. Thyagarajan, K. Gale-Sides, Z. Abdurashidova, J. E. Aguirre, P. Alexander, Z. S. Ali, Y. Balfour, A. P. Beardsley, G. Bernardi, J. D. Bowman, R. F. Bradley, J. Burba, C. Cheng, D. R. DeBoer, M. Dexter, E. de˜Lera˜Acedo, J. S. Dillon, A. Ewall-Wice, G. Fadana, N. Fagnoni, R. Fritz, S. R. Furlanetto, A. Ghosh, B. Glendenning, B. Greig, J. Grobbelaar, Z. Halday, B. J. Hazelton, J. N. Hewitt, J. Hickish, D. C. Jacobs, A. Julius, M. Kariseb, S. A. Kohn, M. Kolopanis, T. Lekalake, A. Liu, A. Loots, D. MacMahon, L. Malan, C. Malgas, M. Maree, Z. Martinot, E. Matsetela, A. Mesinger, M. Molewa, M. F. Morales, A. R. Neben, A. R. Parsons, N. Patra, S. Pieterse, P. La Plante, J. C. Pober, N. Razavi-Ghods, J. Ringuette, J. Robnett, K. Rosie, R. Sell, P. Sims, C. Smith, A. Syce, P. K. ˜G. Williams, and H. Zheng. HI 21cm Cosmology and the Bi-spectrum: Closure Diagnostics in Massively Redundant Interferometric Arrays. ArXiv e-prints, May 2018.

[51] J. S. Dillon, S. A. Kohn, A. R. Parsons, J. E. Aguirre, Z. S. Ali, G. Bernardi, N. S. Kern, W. Li, A. Liu, C. D. Nunhokee, and J. C. Pober. Polarized redundant-baseline calibration for 21 cm cosmology without adding spectral structure. MNRAS, 477:5670–5681, July 2018.

[52] V. Ram Marthi and J. Chengalur. Non-linear redundancy calibration. In Astronomical Society of India Conference Series, volume 13 of Astronomical Society of India Conference Series, pages 393–394, 2014.

[53] J. S. Dillon and A. R. Parsons. Redundant Array Configurations for 21 cm Cosmology. ApJ, 826:181, August 2016.

[54] J. L. Sievers. Calibration of Quasi-Redundant Interferometers. ArXiv e-prints, January 2017.

[55] Naomi Orosz, Joshua S. Dillon, Aaron Ewall-Wice, Aaron R. Parsons, and Nithyanandan Thyagarajan. Mitigating the effects of antenna-to-antenna variation on redundant-baseline calibration for 21 cm cosmology. MNRAS, 487(1):537–549, Jul 2019.

[56] Ruby Byrne, Miguel F. Morales, Bryna Hazelton, Wenyang Li, Nichole Barry, Adam P. Beardsley, Ronniy Joseph, Jonathan Pober, Ian Sullivan, and Cathryn Trott. Fundamental Limitations on the Calibration of Redundant 21 cm Cosmology Instruments and Implications for HERA and the SKA. ApJ, 875(1):70, Apr 2019.

[57] A. R. Offringa, R. B. Wayth, N. Hurley-Walker, D. L. Kaplan, N. Barry, A. P. Beardsley, M. E. Bell, G. Bernardi, J. D. Bowman, F. Briggs, J. R. Callingham, R. J. Cappallo, P. Carroll,

A. A. Deshpande, J. S. Dillon, K. S. Dwarakanath, A. Ewall-Wice, L. Feng, B.-Q. For, B. M. Gaensler, L. J. Greenhill, P. Hancock, B. J. Hazelton, J. N. Hewitt, L. Hindson, D. C. Jacobs, M. Johnston-Hollitt, A. D. Kapińska, H.-S. Kim, P. Kittiwisit, E. Lenc, J. Line, A. Loeb, C. J. Lonsdale, B. McKinley, S. R. McWhirter, D. A. Mitchell, M. F. Morales, E. Morgan, J. Morgan, A. R. Neben, D. Oberoi, S. M. Ord, S. Paul, B. Pindor, J. C. Pober, T. Prabu, P. Procopio, J. Riding, N. Udaya Shankar, S. Sethi, K. S. Srivani, L. Staveley-Smith, R. Subrahmanyan, I. S. Sullivan, M. Tegmark, N. Thyagarajan, S. J. Tingay, C. M. Trott, R. L. Webster, A. Williams, C. L. Williams, C. Wu, J. S. Wyithe, and Q. Zheng. The Low-Frequency Environment of the Murchison Widefield Array: Radio-Frequency Interference Analysis and Mitigation. PASA, 32:e008, March 2015.

[58] A. R. Offringa, J. J. van de Gronde, and J. B. T. M. Roerdink. A morphological algorithm for improving radio-frequency interference detection. A&A, 539:A95, March 2012.

[59] C. M. Trott, C. H. Jordan, S. G. Murray, B. Pindor, D. A. Mitchell, R. B. Wayth, J. Line, B. McKinley, A. Beardsley, J. Bowman, F. Briggs, B. J. Hazelton, J. Hewitt, D. Jacobs, M. F. Morales, J. C. Pober, S. Sethi, U. Shankar, R. Subrahmanyan, M. Tegmark, S. J. Tingay, R. L. Webster, and J. S. B. Wyithe. Assessment of ionospheric activity tolerances for Epoch of Reionisation science with the Murchison Widefield Array. arXiv e-prints, September 2018.

[60] C. H. Jordan, S. Murray, C. M. Trott, R. B. Wayth, D. A. Mitchell, M. Rahimi, B. Pindor, P. Procopio, and J. Morgan. Characterization of the ionosphere above the Murchison Radio Observatory using the Murchison Widefield Array. MNRAS, 471:3974–3987, November 2017.

[61] B. S. Arora, J. Morgan, S. M. Ord, S. J. Tingay, N. Hurley-Walker, M. Bell, G. Bernardi, N. D. R. Bhat, F. Briggs, J. R. Callingham, A. A. Deshpande, K. S. Dwarakanath, A. Ewall-Wice, L. Feng, B.-Q. For, P. Hancock, B. J. Hazelton, L. Hindson, D. Jacobs, M. Johnston-Hollitt, A. D. Kapińska, N. Kudryavtseva, E. Lenc, B. McKinley, D. Mitchell, D. Oberoi, A. R. Offringa, B. Pindor, P. Procopio, J. Riding, L. Staveley-Smith, R. B. Wayth, C. Wu, Q. Zheng, J. D. Bowman, R. J. Cappallo, B. E. Corey, D. Emrich, R. Goeke, L. J. Greenhill, D. L. Kaplan, J. C. Kasper, E. Kratzenberg, C. J. Lonsdale, M. J. Lynch, S. R. McWhirter, M. F. Morales, E. Morgan, T. Prabu, A. E. E. Rogers, A. Roshi, N. U. Shankar, K. S. Srivani, R. Subrahmanyan, M. Waterson, R. L. Webster, A. R. Whitney, A. Williams, and C. L. Williams. Ionospheric Modelling using GPS to Calibrate the MWA. I: Comparison of First Order Ionospheric Effects between GPS Models and MWA Observations. PASA, 32:e029, August 2015.

[62] K. Bandura, G. E. Addison, M. Amiri, J. R. Bond, D. Campbell-Wilson, L. Connor, J.-F. Cliche, G. Davis, M. Deng, N. Denman, M. Dobbs, M. Fandino, K. Gibbs, A. Gilbert, M. Halpern, D. Hanna, A. D. Hincks, G. Hinshaw, C. Höfer, P. Klages, T. L. Landecker, K. Masui, J. Mena Parra, L. B. Newburgh, U.-l. Pen, J. B. Peterson, A. Recnik, J. R. Shaw, K. Sigurdson, M. Sitwell, G. Smecher, R. Smegal, K. Vanderlinde, and D. Wiebe. Canadian Hydrogen Intensity Mapping Experiment (CHIME) pathfinder. In Society of Photo-Optical Instrumentation Engineers (SPIE) Conference Series, volume 9145 of Society of Photo-Optical Instrumentation Engineers (SPIE) Conference Series, page 22, July 2014.

[63] L. B. Newburgh, G. E. Addison, M. Amiri, K. Bandura, J. R. Bond, L. Connor, J.-F. Cliche, G. Davis, M. Deng, N. Denman, M. Dobbs, M. Fandino, H. Fong, K. Gibbs, A. Gilbert, E. Griffin, M. Halpern, D. Hanna, A. D. Hincks, G. Hinshaw, C. Höfer, P. Klages, T. Landecker,

K. Masui, J. M. Parra, U.-L. Pen, J. Peterson, A. Recnik, J. R. Shaw, K. Sigurdson, M. Sitwell, G. Smecher, R. Smegal, K. Vanderlinde, and D. Wiebe. Calibrating CHIME: a new radio interferometer to probe dark energy. In Society of Photo-Optical Instrumentation Engineers (SPIE) Conference Series, volume 9145 of Society of Photo-Optical Instrumentation Engineers (SPIE) Conference Series, page 4, July 2014.

[64] M. Sokolowski, T. Colegate, A. T. Sutinjo, D. Ung, R. Wayth, N. Hurley-Walker, E. Lenc, B. Pindor, J. Morgan, D. L. Kaplan, M. E. Bell, J. R. Callingham, K. S. Dwarakanath, B.-Q. For, B. M. Gaensler, P. J. Hancock, L. Hindson, M. Johnston-Hollitt, A. D. Kapińska, B. McKinley, A. R. Offringa, P. Procopio, L. Staveley-Smith, C. Wu, and Q. Zheng. Calibration and Stokes Imaging with Full Embedded Element Primary Beam Model for the Murchison Widefield Array. PASA, 34:e062, November 2017.

[65] D. C. Jacobs, J. Burba, J. Bowman, A. R. Neben, B. Stinnett, and L. Turner. The External Calibrator for Hydrogen Observatories. ArXiv e-prints, October 2016.

[66] A. R. Neben, R. F. Bradley, J. N. Hewitt, D. R. DeBoer, A. R. Parsons, J. E. Aguirre, Z. S. Ali, C. Cheng, A. Ewall-Wice, N. Patra, N. Thyagarajan, J. Bowman, R. Dickenson, J. S. Dillon, P. Doolittle, D. Egan, M. Hedrick, D. C. Jacobs, S. A. Kohn, P. J. Klima, K. Moodley, B. R. B. Saliwanchik, P. Schaffner, J. Shelton, H. A. Taylor, R. Taylor, M. Tegmark, B. Wirt, and H. Zheng. The Hydrogen Epoch of Reionization Array Dish. I. Beam Pattern Measurements and Science Implications. ApJ, 826:199, August 2016.

[67] G. Virone, A. M. Lingua, M. Piras, A. Cina, F. Perini, J. Monari, F. Paonessa, O. A. Peverini, G. Addamo, and R. Tascone. Antenna pattern verification system based on a micro unmanned aerial vehicle (uav). IEEE Antennas and Wireless Propagation Letters, 13:169–172, 2014.

[68] G. Pupillo, G. Naldi, G. Bianchi, A. Mattana, J. Monari, F. Perini, M. Poloni, M. Schiaffino, P. Bolli, A. Lingua, I. Aicardi, H. Bendea, P. Maschio, M. Piras, G. Virone, F. Paonessa, Z. Farooqui, A. Tibaldi, G. Addamo, O. A. Peverini, R. Tascone, and S. J. Wijnholds. Medicina array demonstrator: calibration and radiation pattern characterization using a uav-mounted radio-frequency source. Experimental Astronomy, 39(2):405–421, Jun 2015.

[69] C. Chang, C. Monstein, A. Refregier, A. Amara, A. Glauser, and S. Casura. Beam Calibration of Radio Telescopes with Drones. PASP, 127:1131, November 2015.

[70] J. L. B. Line, B. McKinley, J. Rasti, M. Bhardwaj, R. B. Wayth, R. L. Webster, D. Ung, D. Emrich, L. Horsley, A. Beardsley, B. Crosse, T. M. O. Franzen, B. M. Gaensler, M. Johnston-Hollitt, D. L. Kaplan, D. Kenney, M. F. Morales, D. Pallot, K. Steele, S. J. Tingay, C. M. Trott, M. Walker, A. Williams, and C. Wu. In situ measurement of MWA primary beam variation using ORBCOMM. PASA, 35, December 2018.

[71] `https://www.intel.com/content/dam/www/programmable/us/en/pdfs/literature/wp/wp-01029.pdf`.

[72] `https://insidehpc.com/2017/12/accelerating-hpc-intel-fpgas/`.

[73] L. R. D'Addario and D. Wang. A low-power correlator asic for arrays with many antennas. In 2016 United States National Committee of URSI National Radio Science Meeting (USNC-URSI NRSM), pages 1–2, Jan 2016.

[74] S. E. Harper and C. Dickinson. Potential impact of global navigation satellite services on total power H I intensity mapping surveys. MNRAS, 479:2024–2036, September 2018.

[75] J. C. Pober. The impact of foregrounds on redshift space distortion measurements with the highly redshifted 21-cm line. MNRAS, 447:1705–1712, February 2015.

[76] A. Liu, A. R. Parsons, and C. M. Trott. Epoch of reionization window. I. Mathematical formalism. Phys. Rev. D, 90(2):023018, July 2014.

[77] J. Jewell, S. Levin, and C. H. Anderson. Application of Monte Carlo Algorithms to the Bayesian Analysis of the Cosmic Microwave Background. ApJ, 609:1–14, July 2004.

[78] Hong-Ming Zhu, Ue-Li Pen, Yu Yu, Xinzhong Er, and Xuelei Chen. Cosmic tidal reconstruction. Phys. Rev., D93(10):103504, 2016.

[79] Simon Foreman, P. Daniel Meerburg, Alexander van Engelen, and Joel Meyers. Lensing reconstruction from line intensity maps: the impact of gravitational nonlinearity. JCAP, 1807(07):046, 2018.

[80] Joshua S. Dillon, Adrian Liu, Christopher L. Williams, Jacqueline N. Hewitt, Max Tegmark, Edward H. Morgan, Alan M. Levine, Miguel F. Morales, Steven J. Tingay, and Gianni Bernardi. Overcoming real-world obstacles in 21 cm power spectrum estimation: A method demonstration and results from early Murchison Widefield Array data. Phys. Rev. D, 89(2):023002, Jan 2014.

[81] D. J. Eisenstein, H.-J. Seo, E. Sirko, and D. N. Spergel. Improving Cosmological Distance Measurements by Reconstruction of the Baryon Acoustic Peak. ApJ, 664:675–679, August 2007.

[82] N. Padmanabhan, M. White, and J. D. Cohn. Reconstructing baryon oscillations: A Lagrangian theory perspective. Phys. Rev. D, 79(6):063523, March 2009.

[83] Carina Cheng, Aaron R. Parsons, Matthew Kolopanis, Daniel C. Jacobs, Adrian Liu, Saul A. Kohn, James E. Aguirre, Jonathan C. Pober, Zaki S. Ali, and Gianni Bernardi. Characterizing Signal Loss in the 21 cm Reionization Power Spectrum: A Revised Study of PAPER-64. ApJ, 868(1):26, Nov 2018.

[84] Francisco Villaescusa-Navarro, Shy Genel, Emanuele Castorina, Andrej Obuljen, David N. Spergel, Lars Hernquist, Dylan Nelson, Isabella P. Carucci, Annalisa Pillepich, Federico Marinacci, Benedikt Diemer, Mark Vogelsberger, Rainer Weinberger, and Rüdiger Pakmor. Ingredients for 21 cm Intensity Mapping. ApJ, 866:135, Oct 2018.

[85] D. Alonso, P. G. Ferreira, and M. G. Santos. Fast simulations for intensity mapping experiments. MNRAS, 444:3183–3197, November 2014.

[86] P. Monaco, E. Sefusatti, S. Borgani, M. Crocce, P. Fosalba, R. K. Sheth, and T. Theuns. An accurate tool for the fast generation of dark matter halo catalogues. MNRAS, 433:2389–2402, August 2013.

[87] F.-S. Kitaura and S. Heß. Cosmological structure formation with augmented Lagrangian perturbation theory. MNRAS, 435:L78–L82, August 2013.

[88] S. Avila, S. G. Murray, A. Knebe, C. Power, A. S. G. Robotham, and J. Garcia-Bellido. HALOGEN: a tool for fast generation of mock halo catalogues. MNRAS, 450:1856–1867, June 2015.

[89] C.-H. Chuang, F.-S. Kitaura, F. Prada, C. Zhao, and G. Yepes. EZmocks: extending the Zel'dovich approximation to generate mock galaxy catalogues with accurate clustering statistics. MNRAS, 446:2621–2628, January 2015.

[90] M. Vakili, F.-S. Kitaura, Y. Feng, G. Yepes, C. Zhao, C.-H. Chuang, and C. Hahn. Accurate halo-galaxy mocks from automatic bias estimation and particle mesh gravity solvers. MNRAS, 472:4144–4154, December 2017.

[91] S. Tassev, M. Zaldarriaga, and D. J. Eisenstein. Solving large scale structure in ten easy steps with COLA. J. Cosmology Astropart. Phys., 6:036, June 2013.

[92] M. White, J. L. Tinker, and C. K. McBride. Mock galaxy catalogues using the quick particle mesh method. MNRAS, 437:2594–2606, January 2014.

[93] Y. Feng, M.-Y. Chu, U. Seljak, and P. McDonald. FASTPM: a new scheme for fast simulations of dark matter and haloes. MNRAS, 463:2273–2286, December 2016.

[94] G. Stein, M.. A. Alvarez, and J. R. Bond. The mass-Peak Patch algorithm for fast generation of deep all-sky dark matter halo catalogues and its N-Body validation. ArXiv e-prints, October 2018.

[95] B. Greig and A. Mesinger. Simultaneously constraining the astrophysics of reionisation and the epoch of heating with 21CMMC. In V. Jelić and T. van der Hulst, editors, Peering towards Cosmic Dawn, volume 333 of IAU Symposium, pages 18–21, May 2018.

[96] A. Lanman, B. Hazelton, D. Jacobs, M. Kolopanis, J. Pober, J. Aguirre, and N. Thyagarajan. pyuvsim: A comprehensive simulation package for radio interferometers in python. The Journal of Open Source Software, 4:1234, May 2019.

[97] G. Prézeau and M. Reinecke. Algorithm for the Evaluation of Reduced Wigner Matrices. ApJS, 190:267–274, October 2010.

[98] A. J. Cianciara, C. J. Anderson, X. Chen, Z. Chen, J. Geng, J. Li, C. Liu, T. Liu, W. Lu, J. B. Peterson, H. Shi, C. N. Steffel, A. Stebbins, T. Stucky, S. Sun, P. T. Timbie, Y. Wang, F. Wu, and J. Zhang. Simulation and Testing of a Linear Array of Modified Four-Square Feed Antennas for the Tianlai Cylindrical Radio Telescope. Journal of Astronomical Instrumentation, 6:1750003–40, September 2017.

[99] M. Deng, D. Campbell-Wilson, and for the CHIME Collaboration. The cloverleaf antenna: A compact wide-bandwidth dual-polarization feed for CHIME. ArXiv e-prints, August 2017.

[100] A. Ewall-Wice, R. Bradley, D. Deboer, J. Hewitt, A. Parsons, J. Aguirre, Z. S. Ali, J. Bowman, C. Cheng, A. R. Neben, N. Patra, N. Thyagarajan, M. Venter, E. de Lera Acedo, J. S. Dillon, R. Dickenson, P. Doolittle, D. Egan, M. Hedrick, P. Klima, S. Kohn, P. Schaffner, J. Shelton, B. Saliwanchik, H. A. Taylor, R. Taylor, M. Tegmark, and B. Wirt. The Hydrogen Epoch of Reionization Array Dish. II. Characterization of Spectral Structure with Electromagnetic Simulations and Its Science Implications. ApJ, 831:196, November 2016.

[101] Gregory Paciga, Joshua G. Albert, Kevin Bandura, Tzu-Ching Chang, Yashwant Gupta, Christopher Hirata, Julia Odegova, Ue-Li Pen, Jeffrey B. Peterson, Jayanta Roy, J. Richard Shaw, Kris Sigurdson, and Tabitha Voytek. A simulation-calibrated limit on the H I power spectrum from the GMRT Epoch of Reionization experiment. MNRAS, 433:639–647, July 2013.

[102] E. R. Switzer, K. W. Masui, K. Bandura, L.-M. Calin, T.-C. Chang, X.-L. Chen, Y.-C. Li, Y.-W. Liao, A. Natarajan, U.-L. Pen, J. B. Peterson, J. R. Shaw, and T. C. Voytek. Determination of z 0.8 neutral hydrogen fluctuations using the 21 cm intensity mapping autocorrelation. MNRAS, 434:L46–L50, July 2013.

[103] Michael W. Eastwood, Marin M. Anderson, Ryan M. Monroe, Gregg Hallinan, Benjamin R. Barsdell, Stephen A. Bourke, M. A. Clark, Steven W. Ellingson, Jayce Dowell, Hugh Garsden, Lincoln J. Greenhill, Jacob M. Hartman, Jonathon Kocz, T. Joseph W. Lazio, Danny C. Price, Frank K. Schinzel, Gregory B. Taylor, Harish K. Vedantham, Yuankun Wang, and David P. Woody. The Radio Sky at Meter Wavelengths: m-mode Analysis Imaging with the OVRO-LWA. AJ, 156(1):32, Jul 2018.

[104] `http://www.tauceti.caltech.edu/LWA/`.

[105] S. J. Tingay, R. Goeke, J. D. Bowman, D. Emrich, S. M. Ord, D. A. Mitchell, M. F. Morales, T. Booler, B. Crosse, R. B. Wayth, C. J. Lonsdale, S. Tremblay, D. Pallot, T. Colegate, A. Wicenec, N. Kudryavtseva, W. Arcus, D. Barnes, G. Bernardi, F. Briggs, S. Burns, J. D. Bunton, R. J. Cappallo, B. E. Corey, A. Deshpande, L. Desouza, B. M. Gaensler, L. J. Greenhill, P. J. Hall, B. J. Hazelton, D. Herne, J. N. Hewitt, M. Johnston-Hollitt, D. L. Kaplan, J. C. Kasper, B. B. Kincaid, R. Koenig, E. Kratzenberg, M. J. Lynch, B. Mckinley, S. R. Mcwhirter, E. Morgan, D. Oberoi, J. Pathikulangara, T. Prabu, R. A. Remillard, A. E. E. Rogers, A. Roshi, J. E. Salah, R. J. Sault, N. Udaya-Shankar, F. Schlagenhaufer, K. S. Srivani, J. Stevens, R. Subrahmanyan, M. Waterson, R. L. Webster, A. R. Whitney, A. Williams, C. L. Williams, and J. S. B. Wyithe. The Murchison Widefield Array: The Square Kilometre Array Precursor at Low Radio Frequencies. PASA, 30:e007, January 2013.

[106] `http://www.mwatelescope.org/science/epoch-of-reionization-eor`.

[107] Aaron R. Parsons, Donald C. Backer, Griffin S. Foster, Melvyn C. H. Wright, Richard F. Bradley, Nicole E. Gugliucci, Chaitali R. Parashare, Erin E. Benoit, James E. Aguirre, Daniel C. Jacobs, Chris L. Carilli, David Herne, Mervyn J. Lynch, Jason R. Manley, and Daniel J. Werthimer. The Precision Array for Probing the Epoch of Re-ionization: Eight Station Results. AJ, 139:1468–1480, April 2010.

[108] `http://eor.berkeley.edu/`.

[109] David R. DeBoer, Aaron R. Parsons, James E. Aguirre, Paul Alexander, Zaki S. Ali, Adam P. Beardsley, Gianni Bernardi, Judd D. Bowman, Richard F. Bradley, Chris L. Carilli, Carina Cheng, Eloy de Lera Acedo, Joshua S. Dillon, Aaron Ewall-Wice, Gcobisa Fadana, Nicolas Fagnoni, Randall Fritz, Steve R. Furlanetto, Brian Glendenning, Bradley Greig, Jasper Grobbelaar, Bryna J. Hazelton, Jacqueline N. Hewitt, Jack Hickish, Daniel C. Jacobs, Austin Julius, MacCalvin Kariseb, Saul A. Kohn, Telalo Lekalake, Adrian Liu, Anita Loots, David MacMahon, Lourence Malan, Cresshim Malgas, Matthys Maree, Zachary Martinot, Nathan Mathison,

Eunice Matsetela, Andrei Mesinger, Miguel F. Morales, Abraham R. Neben, Nipanjana Patra, Samantha Pieterse, Jonathan C. Pober, Nima Razavi-Ghods, Jon Ringuette, James Robnett, Kathryn Rosie, Raddwine Sell, Craig Smith, Angelo Syce, Max Tegmark, Nithyanandan Thyagarajan, Peter K. G. Williams, and Haoxuan Zheng. Hydrogen Epoch of Reionization Array (HERA). Publications of the Astronomical Society of the Pacific, 129:045001, April 2017.

[110] `https://reionization.org/`.

[111] M. P. van Haarlem, M. W. Wise, A. W. Gunst, G. Heald, J. P. McKean, J. W. T. Hessels, A. G. de Bruyn, R. Nijboer, J. Swinbank, R. Fallows, M. Brentjens, A. Nelles, R. Beck, H. Falcke, R. Fender, J. Hörandel, L. V. E. Koopmans, G. Mann, G. Miley, H. Röttgering, B. W. Stappers, R. A. M. J. Wijers, S. Zaroubi, M. van den Akker, A. Alexov, J. Anderson, K. Anderson, A. van Ardenne, M. Arts, A. Asgekar, I. M. Avruch, F. Batejat, L. Bähren, M. E. Bell, M. R. Bell, I. van Bemmel, P. Bennema, M. J. Bentum, G. Bernardi, P. Best, L. Bîrzan, A. Bonafede, A.-J. Boonstra, R. Braun, J. Bregman, F. Breitling, R. H. van de Brink, J. Broderick, P. C. Broekema, W. N. Brouw, M. Brüggen, H. R. Butcher, W. van Cappellen, B. Ciardi, T. Coenen, J. Conway, A. Coolen, A. Corstanje, S. Damstra, O. Davies, A. T. Deller, R.-J. Dettmar, G. van Diepen, K. Dijkstra, P. Donker, A. Doorduin, J. Dromer, M. Drost, A. van Duin, J. Eislöffel, J. van Enst, C. Ferrari, W. Frieswijk, H. Gankema, M. A. Garrett, F. de Gasperin, M. Gerbers, E. de Geus, J.-M. Grießmeier, T. Grit, P. Gruppen, J. P. Hamaker, T. Hassall, M. Hoeft, H. A. Holties, A. Horneffer, A. van der Horst, A. van Houwelingen, A. Huijgen, M. Iacobelli, H. Intema, N. Jackson, V. Jelic, A. de Jong, E. Juette, D. Kant, A. Karastergiou, A. Koers, H. Kollen, V. I. Kondratiev, E. Kooistra, Y. Koopman, A. Koster, M. Kuniyoshi, M. Kramer, G. Kuper, P. Lambropoulos, C. Law, J. van Leeuwen, J. Lemaitre, M. Loose, P. Maat, G. Macario, S. Markoff, J. Masters, R. A. McFadden, D. McKay-Bukowski, H. Meijering, H. Meulman, M. Mevius, E. Middelberg, R. Millenaar, J. C. A. Miller-Jones, R. N. Mohan, J. D. Mol, J. Morawietz, R. Morganti, D. D. Mulcahy, E. Mulder, H. Munk, L. Nieuwenhuis, R. van Nieuwpoort, J. E. Noordam, M. Norden, A. Noutsos, A. R. Offringa, H. Olofsson, A. Omar, E. Orrú, R. Overeem, H. Paas, M. Pandey-Pommier, V. N. Pandey, R. Pizzo, A. Polatidis, D. Rafferty, S. Rawlings, W. Reich, J.-P. de Reijer, J. Reitsma, G. A. Renting, P. Riemers, E. Rol, J. W. Romein, J. Roosjen, M. Ruiter, A. Scaife, K. van der Schaaf, B. Scheers, P. Schellart, A. Schoenmakers, G. Schoonderbeek, M. Serylak, A. Shulevski, J. Sluman, O. Smirnov, C. Sobey, H. Spreeuw, M. Steinmetz, C. G. M. Sterks, H.-J. Stiepel, K. Stuurwold, M. Tagger, Y. Tang, C. Tasse, I. Thomas, S. Thoudam, M. C. Toribio, B. van der Tol, O. Usov, M. van Veelen, A.-J. van der Veen, S. ter Veen, J. P. W. Verbiest, R. Vermeulen, N. Vermaas, C. Vocks, C. Vogt, M. de Vos, E. van der Wal, R. van Weeren, H. Weggemans, P. Weltevrede, S. White, S. J. Wijnholds, T. Wilhelmsson, O. Wucknitz, S. Yatawatta, P. Zarka, A. Zensus, and J. van Zwieten. LOFAR: The LOw-Frequency ARray. A&A, 556:A2, August 2013.

[112] `http://www.lofar.org/astronomy/eor-ksp/epoch-reionization`.

[113] K. Bandura, G. E. Addison, M. Amiri, J. R. Bond, D. Campbell-Wilson, L. Connor, J.-F. Cliche, G. Davis, M. Deng, N. Denman, M. Dobbs, M. Fandino, K. Gibbs, A. Gilbert, M. Halpern, D. Hanna, A. D. Hincks, G. Hinshaw, C. Höfer, P. Klages, T. L. Landecker, K. Masui, J. Mena Parra, L. B. Newburgh, U.-l. Pen, J. B. Peterson, A. Recnik, J. R. Shaw, K. Sigurdson, M. Sitwell, G. Smecher, R. Smegal, K. Vanderlinde, and D. Wiebe. Canadian Hydrogen Intensity Mapping Experiment (CHIME) pathfinder. In Ground-based and Airborne Telescopes V, volume 9145 of Proc. SPIE, page 914522, July 2014.

[114] https://chime-experiment.ca/.

[115] L. B. Newburgh, K. Bandura, M. A. Bucher, T.-C. Chang, H. C. Chiang, J. F. Cliche, R. Davé, M. Dobbs, C. Clarkson, K. M. Ganga, T. Gogo, A. Gumba, N. Gupta, M. Hilton, B. Johnstone, A. Karastergiou, M. Kunz, D. Lokhorst, R. Maartens, S. Macpherson, M. Mdlalose, K. Moodley, L. Ngwenya, J. M. Parra, J. Peterson, O. Recnik, B. Saliwanchik, M. G. Santos, J. L. Sievers, O. Smirnov, P. Stronkhorst, R. Taylor, K. Vanderlinde, G. Van Vuuren, A. Weltman, and A. Witzemann. HIRAX: a probe of dark energy and radio transients. In Ground-based and Airborne Telescopes VI, volume 9906 of Proc. SPIE, page 99065X, August 2016.

[116] https://www.acru.ukzn.ac.za/~hirax/.

[117] S. Das, C. J. Anderson, R. Ansari, J.-E. Campagne, D. Charlet, X. Chen, Z. Chen, A. J. Cianciara, P. Colom, Y. Cong, K. G. Gayley, J. Geng, J. Hao, Q. Huang, C. S. Keith, C. Li, J. Li, Y. Li, C. Liu, T. Liu, C. Magneville, J. P. Marriner, J.-M. Martin, M. Moniez, T. M. Oxholm, U.-l. Pen, O. Perdereau, J. B. Peterson, H. Shi, L. Shu, A. Stebbins, S. Sun, P. T. Timbie, S. Torchinsky, G. S. Tucker, G. Wang, R. Wang, X. Wang, Y. Wang, F. Wu, Y. Xu, K. Yu, J. Zhang, J. Zhang, L. Zhang, J. Zhu, and S. Zuo. Progress in the construction and testing of the Tianlai radio interferometers. In Society of Photo-Optical Instrumentation Engineers (SPIE) Conference Series, volume 10708 of Society of Photo-Optical Instrumentation Engineers (SPIE) Conference Series, page 1070836, July 2018.

[118] http://tianlai.bao.ac.cn/.

[119] Suman Chatterjee and Somnath Bharadwaj. A spherical harmonic analysis of the Ooty Wide Field Array (OWFA) visibility signal. MNRAS, 478(3):2915–2926, Aug 2018.

[120] https://en.wikipedia.org/wiki/Ooty_Radio_Telescope.

[121] R. Battye, I. Browne, T. Chen, C. Dickinson, S. Harper, L. Olivari, M. Peel, M. Remazeilles, S. Roychowdhury, P. Wilkinson, E. Abdalla, R. Abramo, E. Ferreira, A. Wuensche, T. Vilella, M. Caldas, G. Tancredi, A. Refregier, C. Monstein, F. Abdalla, A. Pourtsidou, B. Maffei, G. Pisano, and Y.-Z. Ma. Update on the BINGO 21cm intensity mapping experiment. ArXiv e-prints, October 2016.

[122] http://www.bingotelescope.org/en/.

[123] Heino Falcke, Jinsong Ping, Marc Klein Wolt, and Linjie Chen. Radio Astronomy on and around the moon. In 42nd COSPAR Scientific Assembly, volume 42, pages B3.1–25–18, Jul 2018.

[124] Jiao Zhang, Reza Ansari, Xuelei Chen, Jean-Eric Campagne, Christophe Magneville, and Fengquan Wu. Sky reconstruction from transit visibilities: PAON-4 and Tianlai dish array. MNRAS, 461(2):1950–1966, Sep 2016.

[125] https://www.obs-nancay.fr/-PAON-4-.html?lang=fr.

[126] https://www.skatelescope.org/lfaa/.

[127] Cosmic Visions 21 cm Collaboration, Réza Ansari, Evan J. Arena, Kevin Bandura, Philip Bull, Emanuele Castorina, Tzu-Ching Chang, Simon Foreman, Josef Frisch, Daniel Green, Dionysios Karagiannis, Adrian Liu, Kiyoshi W. Masui, P. Daniel Meerburg, Laura B. Newburgh, Andrej Obuljen, Paul O'Connor, J. Richard Shaw, Christopher Sheehy, Anže Slosar, Kendrick Smith, Paul Stankus, Albert Stebbins, Peter Timbie, Francisco Villaescusa-Navarro, and Martin White. Inflation and Early Dark Energy with a Stage II Hydrogen Intensity Mapping experiment. arXiv e-prints, page arXiv:1810.09572, Oct 2018.